THE ASTROPHYSICAL JOURNAL, 384:508–522, 1992 January 10

ABUNDANCES OF THE HEAVY ELEMENTS IN THE MAGELLANIC CLOUDS. III. INTERPRETATION OF RESULTS

STEPHEN C. RUSSELL
Dublin Institute for Advanced Studies, School of Cosmic Physics, 5 Merrion Square, Dublin 2, Ireland

AND

MICHAEL A. DOPITA
Mount Stromlo and Siding Spring Observatories, Institute of Advanced Studies, The Australian National University, Private Bag, Weston Creek P.O., Canberra, ACT 2611, Australia
Received 1990 June 4; accepted 1991 July 19

ABSTRACT

This paper presents chemical and structural evolutionary models for the Magellanic Clouds assuming bimodal star formation and gas infall. The models are discussed in relation to the observed chemical abundances of the Clouds and are compared with our own Galaxy. The detailed abundances derived from previous work are investigated for any obvious trends with metallicity or differences compared with the Galaxy. Considering all the data, conclusions are drawn on the possible star formation histories of the Magellanic Clouds and the implications for our own Galaxy.

The following conclusions were reached in this work. The interstellar medium (ISM) of the LMC has a mean metallicity 0.2 dex lower than the local Galactic ISM, and the metallicity of the SMC is 0.6 dex lower. However, the interstellar media of both the Magellanic Clouds and the Galaxy have significantly nonsolar elemental ratios. This is most evident when considering the lightest and the heaviest of the elements. The *s*-process appears to have been less effective at forming the heavy neutron-capture elements in the Magellanic Clouds than in the Galaxy. The *r*-process, on the other hand, appears to have been more effective.

Of the light elements, carbon appears to be of normal abundance in the Cloud stars relative to the iron abundance, which is in contrast to the carbon abundances in the H II regions, which appear to be anomalously low. The overall distribution of the lightest elements in the Clouds shows a gradual falling off in the abundances, relative to the Sun, as the atomic number decreases. This is seen not to be the case when the abundances are compared with the local ISM, and suggests that the present ISM in the vicinity of the Sun is material that has fallen in from farther out.

Subject headings: Galaxy: abundances — ISM: abundances — Magellanic Clouds — nuclear reactions, nucleosynthesis, abundances

1. INTRODUCTION

The Magellanic Clouds are in many ways easier to understand as galactic systems than our own Galaxy. This results from the fact that they may be viewed in their entirety with very little dust obscuration, either from the Galaxy or internally, and their distances are well established. Also, they are close enough for their population of gaseous emission objects (H II regions, supernova remnants [SNRs], and planetary nebulae) to be studied in great detail, and, with the present generation of sensitive detectors, the complete populations of supergiants in each Cloud are accessible for detailed analysis. Finally, they appear to be somewhat simpler systems, in that they have no well-defined halo or disk, and they are relatively well mixed by gas motions along their central bars (see Pagel et al. 1978), so that an abundance analysis at any one point should reflect the global abundances of the whole Cloud. Dynamically, however, it must be remembered, the Clouds are quite complex, since we observe them at a time when the SMC is being severely disrupted by the gravitational interaction with the Galaxy (see Mathewson & Ford 1984), and a "bridge" of H I gas is observed to connect the two Clouds.

In our two previous papers in this series, Russell & Bessell (1989, hereafter Paper I) and Russell & Dopita (1990, hereafter Paper II), we reported the results of a program of observations intended to establish the first consistent set of global abundances for both Clouds, covering the range of elements from the very lightest (He, C, N, O) up to some of the heaviest (Nd, Sm) observable. Paper I dealt with the detailed abundance analyses of high-dispersion spectra of samples of medium- to low-luminosity F supergiants in both Magellanic Clouds. Paper II described our analysis of the emission spectra of samples of bright H II regions and SNRs in both Clouds, using the general-purpose modeling code MAPPINGS (see Binette, Dopita, & Tuohy 1985; Evans & Dopita 1985). The SNRs were used to provide an overlap between the otherwise disparate sets of abundances derived from supergiants and H II regions. In this way we were able to ensure that the sets of abundances we derived from all sources, for each Cloud, were consistent over the whole range of atomic mass.

In this paper we attempt to interpret the results of the previous two papers in terms of the star formation histories of the Magellanic Clouds, and the relationships between the chemical evolutionary histories of each of the Clouds and with the solar neighborhood of our Galaxy. In § 2 we describe the overall abundance patterns of the Clouds and discuss how they differ from that of the Sun. In § 3 we describe the models we use to explore the star formation histories and associated elemental enrichment in each of the Clouds. In § 4 we discuss the elemental abundance patterns we have found in the Clouds and compare them with the models described in § 3 and with results from the Galaxy. Finally, in § 5 we summarize our findings and make suggestions for some of the work that needs to be done in this relatively new field of research.

2. THE OVERALL ABUNDANCE PATTERN

In Table 1 we summarize the overall abundances which we have chosen as representative of the Magellanic Clouds, when due consideration has been given to all sources of data, from the literature as well as from our own work (Papers I and II). Column (3) gives the abundances by number for the Sun from Cameron (1982b) (except where mentioned), on a scale of $12 + \log N(\mathrm{M/H})$. In column (4) we give the abundances of the local interstellar medium (ISM) relative to the Sun, where the elements heavier than $Z = 18$ and the lighter elements C, Na, Mg, Al, and Si are all derived from Canopus (Lyubimkov & Boyarchuk (1982) in preference, and otherwise from Desikachary & Hearnshaw (1982) or the more recent paper by Reynolds, Hearnshaw, & Cottrell (1988), while the remaining elements come from the work on Galactic H II regions by Shaver et al. (1983). Canopus was chosen to represent stellar population of the present-day ISM, since it is a young, well-studied supergiant, of the same type as the Magellanic Cloud stars studied in Paper I (see Paper I for a more detailed discussion). Columns (5) and (7) give the absolute abundances of the LMC and the SMC, respectively, on the same scale as for the Sun, while the errors deduced from the scatter in the abundances are included in the adjacent columns for each Cloud. Finally, the last two columns give the abundances of the LMC and SMC, respectively, relative to the local ISM as given in column (4). These latter abundances should be less affected by systematic errors in the analyses than the absolute abundances given in columns (5) and (7), since we compare like objects. The heavy-element abundances in columns (5), (7), (9), and (10), for $Z > 18$, and the elements C, Na, Mg, Al, and Si, are derived from the F supergiants studied in Paper I, supplemented by the abundances of the three SMC supergiants analyzed by Spite, Spite, & François (1989) and Spite, Barbuy, & Spite (1989a). The other elements are derived from our work on H II regions and SNRs (Paper II), with due consideration given to the abundances derived in the review by Dufour (1984) from all previous abundance estimates given in the literature.

In Figures 1*a* and 1*b* we plot against atomic number the LMC abundances relative to the Sun and to the local Galactic ISM, respectively (as given in Table 1). Similarly, in Figures 2*a* and 2*b* we plot the results for the SMC. In each case the filled triangle represents the value for carbon derived from the UV observations of H II regions by Dufour, Shields, & Talbot (1982) and Dufour, Schiffer, & Shields (1984); the open circles represent elements with insufficient information for us to

TABLE 1

ADOPTED ABUNDANCES

Element (1)	Z (2)	Sun (3)	Solar Vicinity minus Sun (4)	LMC (5)	σ_{LMC} (6)	SMC (7)	σ_{SMC} (8)	LMC minus Solar Vicinity (9)	SMC minus Solar Vicinity (10)
He	2	10.99[a,b]	0.01	10.94	0.03	10.91	0.05	−0.06	−0.09
C	6	8.62	−0.29	8.04	0.18	7.73	0.13	−0.29	−0.60
N	7	7.94	−0.37	7.14	0.15	6.63	0.20	−0.43	−0.94
O	8	8.84	−0.14	8.35	0.06	8.03	0.10	−0.35	−0.67
Ne	10	7.99[b]	−0.09	7.61	0.05	7.27	0.20	−0.29	−0.63
Na	11	6.35	0.23	7.15:	...	5.96	0.24	0.57:	−0.62
Mg	12	7.60	−0.03	7.47	0.13	6.98	0.12	−0.10	−0.59
Al	13	6.50	0.20[c]	...	...	6.40:	...	...	−0.30:
Si	14	7.58	0.05	7.81:	...	7.03	0.18	0.18:	−0.60
S	16	7.27	−0.21	6.70	0.09	6.59	0.15	−0.36	−0.47
Cl	17	5.25	−0.09	4.76	0.08	4.70	0.20	−0.40	−0.46
Ar	18	6.60[b]	−0.18	6.29	0.25	5.81	0.08	−0.13	−0.61
Ca	20	6.37	−0.25	5.89	0.16	5.69	0.20	−0.23	−0.43
Sc	21	3.07	−0.22	2.64	0.21	2.33	0.15	−0.21	−0.52
Ti	22	5.08[d]	−0.10	4.81	0.07	4.49	0.15	−0.17	−0.49
V	23	3.98	−0.10	4.08	0.16	3.54	0.27	0.20	−0.34
Cr	24	5.68	−0.11	5.47	0.09	5.10	0.20	−0.10	−0.47
Mn	25	5.54	−0.14	5.21	0.21	5.03	0.31	−0.19	−0.37
Fe	26	7.53	−0.11	7.23	0.14	6.84	0.13	−0.19	−0.58
Ni	28	6.25	0.00	6.04	0.09	5.85	0.20	−0.21	−0.41
Cu	29	4.31	−0.18	...	...	3.73:	...	...	−0.40:
Zn	30	4.68	−0.01	4.28	0.10	...	...	−0.39	...
Sr	38	2.93	−0.15	2.47	0.58	1.33	...	−0.31	−1.45:
Y	39	2.26	−0.08	1.93	0.10	1.65	0.23	−0.25	−0.53
Zr	40	2.65	−0.15	2.26	0.17	1.99	0.22	−0.24	−0.51
Ba	56	2.26	0.00	2.03	0.24	1.32	0.48	−0.23	−0.94
La	57	1.14	−0.05	1.07	0.09	0.85	0.29	−0.02	−0.24
Ce	58	1.65	−0.06	1.52	0.09	1.33	0.27	−0.07	−0.26
Nd	60	1.47	0.11	1.68	0.19	1.49	0.12	0.10	−0.09
Sm	62	0.96	−0.14	0.93	0.18	1.08	0.39	0.11	0.26
Eu	63	0.55	−0.13[c]	...	...	0.28	0.08	...	−0.14

[a] Taken from Anders & Grevesse 1989.

[b] The derivation of this value depends, at least partially, on extrasolar sources (e.g., H II regions and hot stars). Therefore, a comparison between solar and extrasolar abundances is not meaningful in this case.

[c] Taken from Spite et al. 1989b.

[d] Taken from Blackwell, Shallis, & Simmons 1982.

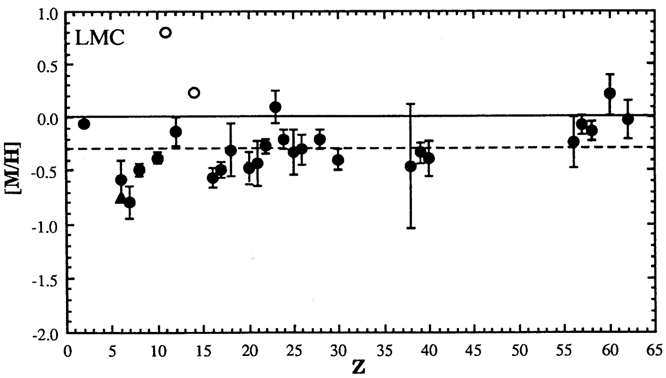

FIG. 1*a*

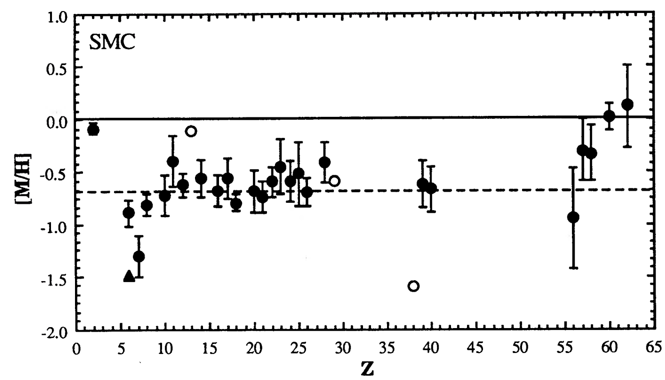

FIG. 2*a*

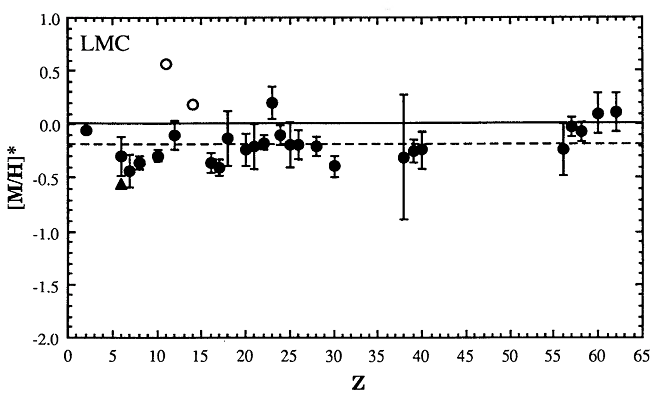

FIG. 1*b*

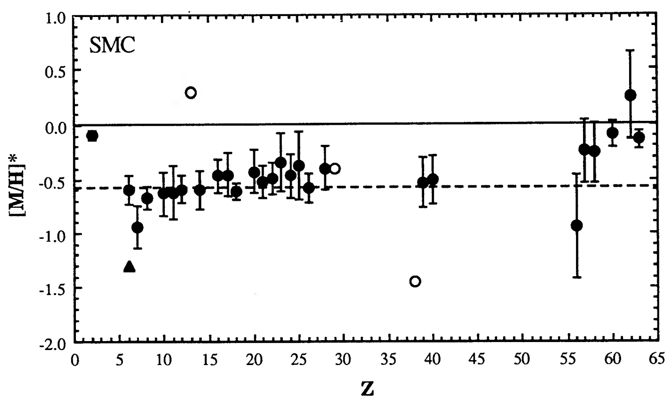

FIG. 2*b*

FIG. 1.—(*a*) Adopted distribution of abundances in the LMC relative to the Sun. The dashed line represents the approximate metallicity of the Cloud. The filled triangle is the C abundance derived from Dufour, Shields, & Talbot (1982) and Dufour, Schiffer, & Shields (1984), and the open circles are elements with insufficient data for an error bar to be estimated. (*b*) Same as (*a*), except that the abundances are relative to the local ISM rather than the Sun, so we define $[M/H]^* = \log_{10} N(M/H)_{object} - \log_{10} N(M/H)_{ISM}$.

FIG. 2.—(*a*) Same as Fig. 1*a*, but for the SMC. (*b*) Same as Fig. 1*b*, but for the SMC.

assign an error bar; and the dashed line represents the approximate Fe abundance.

As noted in Paper I, and shown even more clearly here, there appears to be a pronounced underabundance relative to the Sun for the very lightest elements (Figs. 1*a* and 2*a*). Disregarding the N abundance, which, considering the uncertainties in our present understanding of its formation, is possibly misleadingly low, it is clear that the relative abundances of the three well-observed elements C, O, and Ne are anomalously low compared with those of the heavier elements. Helium is not included in this trend because of its largely cosmic origin. This trend, however, disappears when the abundances are plotted relative to the local ISM (Figs. 1*b* and 2*b*). All three of the critical elements in both Clouds show entirely normal relative abundances. This represents significant evidence that the star formation histories of the Magellanic Clouds are more similar to the star formation history of the *present-day* ISM in the vicinity of the Sun than to that of the Sun itself (see also Peimbert 1987).

The implication of this result is that the Sun was born in a cloud in which more light elements were produced than in the case for the present-day local ISM. Since the Galactic disk may behave a little like an accretion disk, it is possible that the gaseous material from which the Sun was formed has since fallen more toward the center of the Galaxy, while clouds from farther out, where the star formation has not been so intense, have fallen in to the present vicinity of the Sun. If correct, this would represent new evidence for the reality of radial inflow.

The mechanisms that could be responsible for driving the radial inflow of gas in our Galaxy have been discussed in some detail by Dopita (1990). It would appear that stellar orbital diffusion, through gravitational scattering by giant molecular clouds, is the most likely driving force. Since the stellar disk is being heated at a constant rate, and the cloud-star interaction is energy-conserving, the gaseous component must be losing energy. The flat Galactic rotation curve implies that the inflow rate is proportional to the relative surface densities of the stars and the gas. This process is essentially one of dynamical friction, whereby asymmetric drift of the old stars puts a torque on the gas layers which causes them to shed orbital energy and spiral towards the center.

The other major feature of the plots of the overall abundances is the pronounced increase in the very heavy metals ($Z > 56$) with increasing atomic number. This will be discussed in a later section.

3. STAR FORMATION MODELS

3.1. *The Structural Evolution*

We present here possible evolutionary models for the SMC and the LMC and compare the results with the model for the

Galaxy derived by Dopita (1990) using the same code. Since there is no reason to suppose that the solar neighborhood is in any way peculiar in its properties, we might hope that a model which can account for the chemical evolutionary properties of the local environment should be equally capable of accounting for the chemical evolutionary properties of external galaxies.

To this end, a modeling code was developed along the lines described by Matteucci & Tornambè (1985) and Matteucci & Greggio (1986). The code calculates, at each time step, the total amount of infallen gas; the number of stars that are formed within each 0.03 log mass bin, over a specified range of masses (the models being insensitive to the exact mass limits); the number of stars in each mass bin that die and the gas they return to the ISM, and the remnants they leave behind in the form of white dwarfs or neutron stars; and the enrichment or dilution of the ISM that occurs through the ejection of both processed and unprocessed gas from each stellar mass. Any ejected matter is assumed to be made available for further star formation during the following time step. The variation of the chemical yields with metallicity for the massive stars is taken into account, but radial flows are not. The endpoints for the models are constrained by the observations of the ratio of the gas mass to the total mass, the age of the system, the star formation rate, and the oxygen-to-iron abundance ratio. The derived model parameters are given in Table 2, as well as the observationally determined parameters from the literature and the model results for the Galaxy from Dopita (1990). The parameters listed in boldface type represents those that we have chosen specifically to fit with our models.

In these models, we assume in effect that star formation takes place in two quite separate environments. The consequence of this is a bimodal form of the initial mass function (IMF) (the number of stars born per square kiloparsec per year per [log $(M/M_\odot)$]), similar to those proposed by Güsten & Mezger (1983), Larson (1986), and Wyse & Silk (1989). The high-mass star formation applies above $\sim 1\ M_\odot$ and determines the chemical enrichment of the ISM, while the low-mass star formation applies below 1 $M_\odot$ and serves only to lock up gas in long-lived stars. The ratio of the two rates of star formation is detailed as a free parameter; however, since the evolutionary models are relatively insensitive to this parameter, we have retained the value of 4.0 derived for the Galaxy by Dopita (1990).

The logic in favor of adopting a bimodal star formation rate is derived from several physical arguments. If CO–emitting molecular clouds map out the Galactic star-forming regions, then their distribution offers strong support for star formation occurring at two quite different sites. The CO clouds are clearly divided into two populations which reflect their kinetic temperatures. The warm-core (~ 100 K) giant molecular clouds trace the spiral structure of the Galaxy (Güsten & Mezger 1983) and are associated with H II regions, whereas the cold-core (~ 5–15 K) clouds are distributed smoothly throughout the Galaxy (Scoville, Sanders, & Clemens 1986; Scoville & Good 1989).

In the warm-core clouds it is believed that the higher mass stars form preferentially, since the critical mass for fragmentation depends strongly on the gas temperature (Larson 1985). The association of these clouds with spiral arms suggests that cloud-cloud collisions or coalescences provide a heating mechanism for the clouds and the compression necessary to trigger massive star formation within them. Further evidence for this mode of star formation comes from starburst galaxies, where several analyses suggest that *only* high-mass stars are being formed and that the low-mass cutoff in the IMF is of order 3 $M_\odot$ (Rieke et al. 1980, 1985; Olofsson, Bergvall, & Ekman 1984; Augarde & Lequeux 1985).

Although high-mass star formation may dominate in the very earliest stages of development of a normal galaxy (as shown, for instance, in the models of Dopita 1990), the bulk of star formation in mature galaxies is believed to take place in the cold-core molecular clouds, forming stars at a steady rate determined by gravitational fragmentation, and the repressurization of the ISM by the T Tauri winds from low-mass (<1 $M_\odot$) stars as they form (Norman & Silk 1980; Franco 1983; Franco & Cox 1983). Support for this scenario comes from the

TABLE 2

PHYSICAL PARAMETERS

Parameter	Galaxy (Dopita 1989)	SMC Literature	SMC Model	LMC Literature	LMC Model	Reference
IMF exponent p	1.8	2.14	2.32	2.29	2.20	Humphreys & McElroy 1984
Total mass of system ($10^9\ M_\odot$)	400.0	1.8	...	6.1	...	Lequeux 1984
Distance to system (kpc)	...	70.0	...	52.0	...	Lequeux 1984
Radius of system (kpc)	12.5	3.1	...	3.8	...	Mathewson & Ford 1984
Total mass surface density ($M_\odot$ pc^{-2})	70.0	50.0	50.0	130.0	130.0	Derived
Total gas mass ($10^9\ M_\odot$)	28.0	0.65	...	0.70	...	Lequeux 1984
Ratio of gas mass to total mass	**0.07**	**0.36**	**0.36**	**0.11**	**0.11**	Derived
Evolution time (Gyr)	14.8	10.0	8.0	10.0	8.0	Frantsman 1988
Gas depletion time scale (Gyr)	3.5	1.7–6.0	2.9	0.6–1.5	1.85	Dopita 1987 and references therein
Gas infall time scale (Gyr)	1.0	...	3.0	...	3.0	Model
Peak of star formation (Gyr from present)	**12.9**	**2.0–4.0**	**3.6**	**4.0–7.0**	**5.1**	Dopita 1987 and references therein
Low- to high-mass SFR ratio	4.0	...	4.0	...	4.0	Model
Lifetime of binaries, $t_{\rm defl}$ (Gyr)	1.0	...	1.5	...	1.1	Model
% of stars forming binaries	2.0	...	2.5	...	2.0	Model
N(He/H)	0.11	0.081	0.082	0.089	0.091	This work
[C/H]	0.30	−0.86	−0.83	−0.58	−0.32	This work
[N/H]	0.22	−1.31	−0.62	−0.80	−0.24	This work
[O/H]	**0.10**	**−0.77**	**−0.76**	**−0.44**	**−0.44**	This work
[Fe/H]	**0.29**	**−0.65**	**−0.64**	**−0.30**	**−0.30**	This work

NOTE.—The fitted parameters are given in bold type.

scaling relationships observed for the cold-core clouds between the virial mass and the radius, $M_{\rm vir} \propto R^2$, and between the turbulent velocity and the radius, $\Delta v \propto R^{1/2}$ (Larson 1981). Chièze (1987) has shown that this is exactly what would be expected if the clouds were close to gravitational instability in a constant-pressure environment.

The form of the low-mass component is unimportant, since it has no effect on the chemical evolution. The form adopted for the high-mass component is

$$dN/d\,(\log M) = a\{1 - \exp\,[-(M - M_{\rm low}/2)/2M_{\rm low}]\}M^{-p}\ ,$$

where the lower mass cutoff $M_{\rm low}$ is chosen to give a peak near 1 $M_\odot$ and to truncate the IMF below 0.5 $M_\odot$. The exact form of this truncating function is unimportant for chemical evolution, since the lowest mass stars have very little influence on the chemical production matrix. At high masses this function assumes a simple power law, and it is the slope p that is fundamental for stellar nucleosynthesis. In any case, this parameter is all that can be measured with any degree of completeness in the Magellanic Clouds. In the solar neighborhood, the high-mass slope of the IMF is fairly well determined by observation to lie in the range $1.5 \le p \le 2.0$ (Burki 1977; Scalo 1986; Clouds the slope is somewhat steeper (Humphreys & McElroy 1984).

The high-mass star formation rate (SFR) is determined by the monentum balance in cloud-cloud collisions (see Dopita 1990), so that, at any particular time t,

$$\mathrm{SFR}(t) = bM_{\rm gas}^{4/3}\,M_{\rm tot}^{1/3}\ ,$$

where $M_{\rm gas}$ is the surface mass of gas (in $M_\odot$ pc^{-2}), $M_{\rm tot}$ is the total surface mass of the material that has already fallen in, and the constant b is given

$$b = [\tau_{\rm depl}(1 + c)]^{-1}\ ,$$

where $\tau_{\rm depl}$ is the gas depletion time scale, which is defined as the instantaneous gas mass divided by the rate of high-mass star formation, and c is the ratio of the low-mass to the high-mass star formation rate mentioned previously.

The total surface mass of the star-forming region is assumed to be initially zero, and to have increased as a result of infalling, zero-metallicity gas according to

$$M_{\rm tot} = M_T[1 - \exp\,(-t/\tau_{\rm inf})]\ ,$$

where M_T is the total surface mass of the system (determined from Lequeux 1979, 1984) and $\tau_{\rm inf}$ is the gas infall time scale. Although corrections have been made for the helium content, the estimates of the gas surface densities given in Table 2 are probably lower bounds, since there is an unknown degree of saturation in the 21 cm line used in determining the H I surface density, and the contribution due to molecular hydrogen has been ignored. This last factor is probably not serious, however, since both dust and the CO surface density are observed to be low in the Clouds (see Israel 1984 for a full discussion).

The gas infall time scale is loosely constrained by the free-fall collapse time scale of the galaxy. This time scale, $\tau_{\rm ff}$, is given by

$$\tau_{\rm ff} = 1.65(R_{100}/M_{11})^{1/2}\ \mathrm{Gyr}\ ,$$

where R_{100} is the protogalactic radius in units of 100 kpc, and M_{11} is the galaxian mass in units of 10^{11} $M_\odot$ (Dopita 1987). For the Clouds this value is estimated to be between $\sim$2 and 6 Gyr. However, there is the added constraint that the peak gas density occurs at the time of greatest star formation. This results from the strong observational correlation, noted by Dopita (1985), between the specific rate of star formation of massive stars and the gas fraction, in the large sample of irregular and spiral galaxies observed by Donas & Deharveng (1984).

We avoid using the instantaneous recycling approximation, since this is inaccurate for stars with lifetimes of the order of the gas depletion time scale. We therefore adopt the stellar lifetimes suggested by I. Iben (1987, private communication):

$$\tau^* = \begin{cases} 2.64 \times 10^9\ m^{-2.16}\ \mathrm{yr}, & m > 2.3\ M_\odot,\\ 1.1 \times 10^{10}\ m^{-3.50}\ \mathrm{yr}; & m < 2.3\ M_\odot\ . \end{cases}$$

If the stellar lifetime is less than one time step (0.15 Gyr) in computing the models, we assume that the stars die instantaneously and return the appropriate amount of heavy elements to the ISM.

The derived model parameters are given in Table 2, as well as the observationally determined parameters from the literature and the model results for the Galaxy from Dopita (1990). The parameters listed in boldface type represent those that we have chosen specifically to fit with our models.

The models were calculated over an assumed evolutionary time for each of the Clouds, which was initially taken to be 10 Gyr, the age of the oldest known objects in each system (see references quoted in Table 2). However, more accurate models were obtained by assuming an age of 8 Gyr for the Clouds, which probably better reflects the beginning of disk collapse in each Galaxy. Our models are therefore incapable of predicting anything older than 8 Gyr, and on those grounds they are possibly inaccurate (since, as shown in Table 2, the ages for some stars are estimated to be of the order of 10 Gyr). Most likely, this is telling us that the star formation law for the Clouds is somewhat more complex than we have assumed, especially in the period of the slow collapse of the halo. Further modeling shows, however, that the absolute age of the system (within plausible bounds) does not seriously affect the major results derived from the models.

3.2. *The Nucleosynthesis Prescriptions*

Stars can be divided up into three groups by mass, defined according to their ultimate fate as determined by current stellar evolution theory. The most massive stars ($M > 12\ M_\odot$) die as Type II supernovae, and are the main source of heavy elements such as O, Ne, the α-elements, and the r-process elements (Arnett 1978; Woosley & Weaver 1982, 1986; Thielemann & Arnett 1985). The least massive stars are assumed to have an upper limit of 5 $M_\odot$ (see, for instance, Tosi & Diaz 1985), which is "classically" thought to be the upper mass limit for stars incapable of igniting carbon in an electron-degenerate core. These stars end their lives by ejection of their outer shells to form planetary nebulae, and leave behind a white dwarf. The nucleosynthesis prescription of Renzini & Voli (1981), with a mass-loss parameter of $\eta = 0.33$ and a mixing-length parameter $\alpha = 1.5$, has been used in this mass range. These stars contribute to the enrichment of the ISM mainly through the production of ^{4}He, ^{12}C, ^{13}C, ^{14}N, and the s-process elements (Dopita & Meatheringham 1991a, b).

In the mass range from 5 to 12 $M_\odot$, the ultimate fate of the stars is still somewhat controversial. Up to a mass of $\sim$8 $M_\odot$, the stars are theoretically capable of building electron-degenerate C-O cores having masses up to the Chandrasekhar limit (see Nomoto, Thielemann, & Yoloi 1984; Thielemann, Nomoto, & Yokoi 1986), in which case they would explode by detonation or carbon deflagration. Both scenarios would result in total disruption of the star; however, the former is rendered less likely because of the large overabundance of Fe expected if they occur in appreciable numbers (see Audouze, Chiosi, & Woosley 1986). The carbon deflagration supernovae would produce a range of possible nucleosynthetic prescriptions depending on the velocity of the deflagration wave, and would by and large mimic the effects of the deflagration of binary C-O white dwarfs (discussed further on). With the inclusion of convective overshooting in stellar model calculations, however, the mass range where single-star deflagration is possible may be reduced to insignificant levels (Matteucci & Tosi 1985; Castellani et al. 1985; Renzini et al. 1985), and it may be that stars of 6–8 $M_\odot$ actually produce Type II supernovae as suggested by Tornambè & Matteucci (1987).

The fate of stars in the mass range 8–12 $M_\odot$ has been reviewed by Nomoto (1984). They are thought to collapse as a result of electron captures in the core, and if the explosions resulting from this do not totally disrupt the star, the ejecta probably make no significant contribution to the enrichment of the ISM, owing to the small amount of heavy-element–enriched matter overlying the degenerate O/Ne/Mg core.

Owing to the present uncertainties involved in modeling the whole mass range from 5 to 12 $M_\odot$, we assume for our models the nucleosynthetic prescriptions of Renzini & Voli (1981) for $5 < M/M_\odot < 8$, whereby these stars end their lives by ejecting only their outer envelope, leaving behind a white dwarf. The contributions from the mass range $8 < M/M_\odot < 12$ are assumed to be negligible.

The mass (in solar masses) of the remnants $m_{\rm rem}$, assumed to be left behind after the death of a single star of any mass, is based on the work of Iben & Tutukov (1985) and Arnett (1978):

$$m_{\rm rem} = \begin{cases} 0.35 + 0.22m, & m < 5\ M_\odot, \\ 1.42, & 5M_\odot < m < 12\ M_\odot, \\ 1.42 + 0.01(m - 11.5), & m > 12\ M_\odot. \end{cases}$$

All stars in the mass range $3 < M/M_\odot < 12$ may, however, still end their lives as supernovae, if they form part of a binary system. The most successful models for the progenitors of Type Ia supernovae assume that they originate from the carbon deflagration of C-O white dwarfs in a binary system (Whelan & Iben 1973; Iben & Tutukov 1984, 1985). These would result in the total disruption of the star and the ejection of large amounts of Fe and lesser, but still significant, amounts of the elements from Si to Ca (see Nomoto et al. 1984, case C6, and Thielemann et al. 1986).

Type Ib supernovae could also result from C-O white dwarfs in binary systems, in this case by an off-center He detonation (Branch & Nomoto 1986; Iben et al. 1987; Tornambè & Matteucci 1987), although there is some suggestion that these supernovae arise from the explosion of Wolf-Rayet stars (Gaskell et al. 1986; Filippenko & Sargent 1986). This type of supernova is, however, relatively rare, forming just 10% of all Type I supernovae (Audouze et al. 1986), and at this level of accuracy can easily be ignored.

It is difficult to model the exact range of semimajor axes that might occur in C-O binary pairs, and hence the delay before they would coalesce. We simplify the problem by assuming that some fraction, taken to be a free variable in the range ~1–4%, of all white dwarfs form Type I supernova precursors, and that an exponentially decaying fraction of these deflagrate as time passes. This approach involves fewer variables, but it may be somewhat less accurate in principle than the approach of Matteucci & Greggio (1986). Satisfactory models for the Galaxy were produced by Dopita (1990) adopting the precursor fraction to be 2%. Although this figure is not well constrained, it is in agreement with the expected number of Type I supernovae for the Galaxy (van den Bergh, McClure, & Evans 1987), which also results in 2% (with an estimated error of a factor of 2) of the expected number of white dwarfs (if we assume each white dwarf to be 1.4 $M_\odot$).

3.3. *Star Formation*

In Figure 3*a* we show the evolution of the gas surface mass density and of the stellar surface mass density, relative to the total surface mass density of the complete system, for our models of both the SMC and the LMC. This may be compared with the Galactic model derived by Dopita (1990), which is

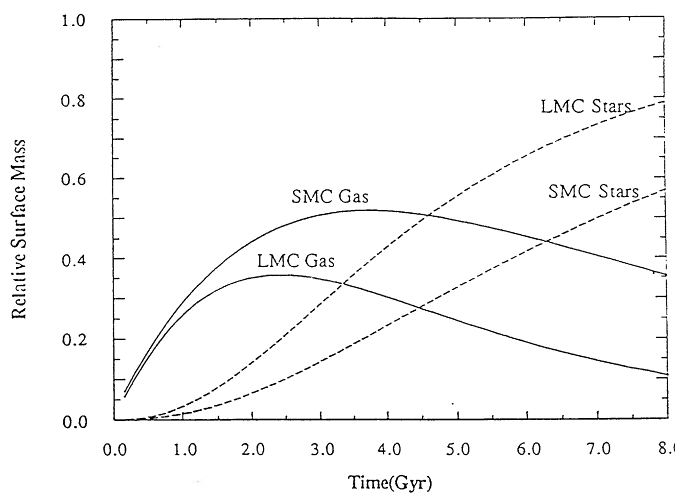

FIG. 3*a*

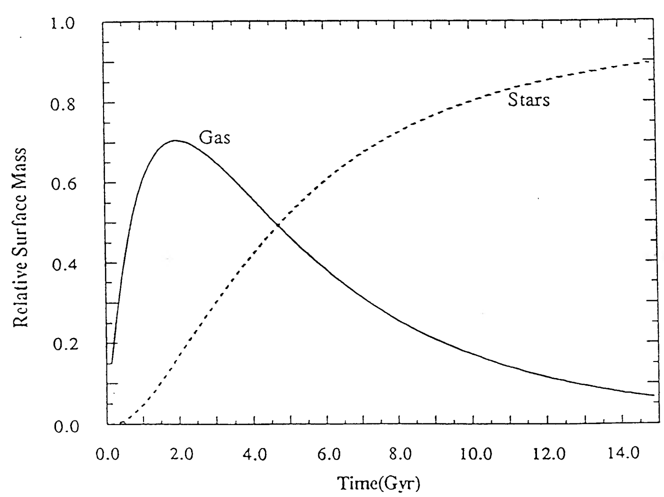

FIG. 3*b*

FIG. 3.—(*a*) Gas surface mass density relative to the total systemic mass for the SMC and the LMC (*solid lines as marked*) and star surface mass density relative to the total systemic mass for the Clouds (*dashed lines as marked*), plotted against time. (*b*) Same as (*a*), but for the Galaxy.

given here in Figure 3*b*. We can immediately see that the peak in gas mass, and hence the star formation rate, monotonically broadens as the surface density of the galaxy decreases, as well as being progressively further delayed in time. This fits in well with the observations for all three galaxies. The observations of our own Galactic neighborhood can best be modeled on the basis of a prompt initial enrichment (see, for instance, Pagel 1988), which requires a narrow intense peak in star formation very early in the history of the Galaxy. Such a peak is a prominent feature of the model shown in Figure 3*b*. On the other hand, the LMC is observed to have a broader star formation peak at a look-back time of around 5 Gyr (see Butcher 1977; Stryker 1981; Stryker & Butcher 1981; Frogel & Blanco 1983), and for the SMC there is some question whether any peak can be observed at all (see Bica, Dottori, & Pastoriza 1986; Frantsman 1988). If there is one, it is probably at a look-back time of around 3 Gyr (see Hawkins & Brück 1982, 1984). The peaks in the star formation rate were specifically fitted in our models, but they successfully predict the increasing *definition* of the peak with increasing galactic disk surface density.

The specific star-forming efficiencies, defined here as being the mass of stars formed at a given time divided by the total systemic mass, do not show a monotonic trend. The LMC and the Galaxy appear to have very similar specific star-forming efficiencies at 8 Gyr. The SMC, on the other hand, is significantly less efficient at producing stars, and a greater specific surface density of gas is allowed to build up in this galaxy than in the more massive LMC. This suggests the possible scenario whereby the disk of any galaxy is equally efficient at forming stars, as long as it exceeds some critical surface mass density. Thus, for less massive galaxies the star formation efficiency is expected to decrease progressively, while the gas content increases. This conjecture was tested using the sample of irregular galaxies studied by Hunter, Gallagher, & Rautenkranz (1982), as well as for the Galaxy and the Magellanic Clouds. In Figure 4 we plot the observed ratio of the star mass to the total mass against the total mass. A least-squares second-order fit has been drawn through the data, and, although the scatter is substantial (owing, at least in part, to the large observational error inherent in the estimation of mass), the data are not inconsistent with our conjecture.

3.4. *Chemical Evolution*

We have specifically modeled the abundance variations of He, C, N, O, and Fe. These elements encompass the three main sources of chemical enrichment: C and N are produced in the low- to intermediate-mass range, O is produced in massive stars ($\geq 12\ M_\odot$), and Fe is produced mainly from Type Ia supernovae, but with a significant contribution ($\sim\frac{1}{3}$) from Type II supernovae. Included in the Fe-peak elements and sharing the evolution of Fe would be Cr and Ni (and to some extent Zn), whereas enrichment of the α-elements, Ne, Mg, S, Si, Ca, and Ti, would be expected to follow the evolution of O.

The low-abundance asymptotic value for the [O/Fe] ratio, where we use the usual notation

$$[\mathrm{M/X}] = \log_{10} N(\mathrm{M/X})_{\mathrm{object}} - \log_{10} N(\mathrm{M/X})_\odot ,$$

puts strong constraints on the production of iron in normal Type II supernovae (since the lower mass precursors of Type Ia supernovae have not had a chance to evolve). As discussed by Dopita (1990), the explosion of SN 1987A allows us to estimate the value of this ratio. This supernova produced a ratio of $[\mathrm{O/Fe}] = 0.65 \pm 0.25$, which is very similar to the value observed in extreme Population II halo stars in the Galaxy, $[\mathrm{O/Fe}] = 0.5 \pm 0.2$ (Sneden 1985; Wheeler, Sneden, & Truran 1989), suggesting that such Type II supernovae may have dominated the nucelosynthesis during the collapse phase of our Galaxy.

The evolution of [O/Fe] with metallicity is driven by the slope of the IMF and by the relevant time scales; the time scale for the infall of halo gas and the deflagration time scale. The deflagration time scale (τ_{defl}) is the characteristic time between the formation of a white dwarf and its subsequent deflagration, and it depends critically (to the fourth power) on the semimajor axis of the precursor binary system (Iben & Tutukov 1984; Matteucci & Greggio 1986). Models of the solar neighborhood by Dopita (1990) indicate that the observed abundance ratios of the α-elements relative to Fe as a function of [Fe/H] (see Fig. 5), are best fitted assuming a deflagration time scale of the order of $1.0^{+1.5}_{-0.5}$ Gyr. An overestimate in the deflagration time scale gives too long a delay before Fe enrichment from Type I supernovae starts to take effect and the slope of the increase in the [α/Fe] ratio becomes too steep. At times long compared to

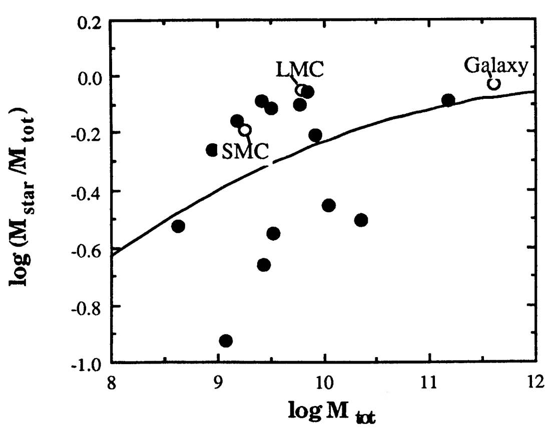

FIG. 4.—Stellar mass fraction of the total systemic mass plotted against the total systemic mass, for the Galaxy and the Magellanic Clouds (*open circles as marked*) and for the sample of irregular galaxies from Hunter, Gallagher, & Rautenkranz (1982) (*filled circles*). The line represents a least-squares second-order fit to the data.

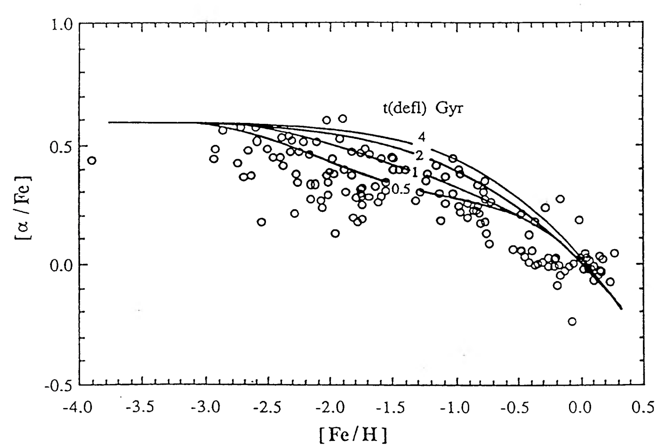

FIG. 5.—Illustration (from Dopita 1990) of the fits of several models with different deflagration time scales τ_{defl} (in Gyr) to the collected Galactic data on the [α-elements/Fe] ratio plotted against [Fe/H] (from Wheeler, Sneden, & Truran 1989).

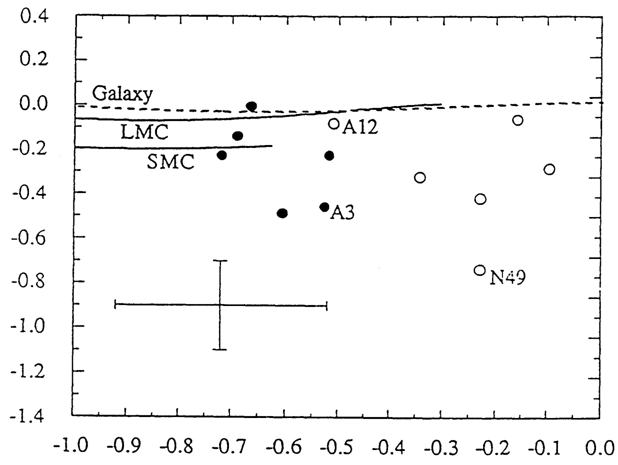

FIG. 6*a*

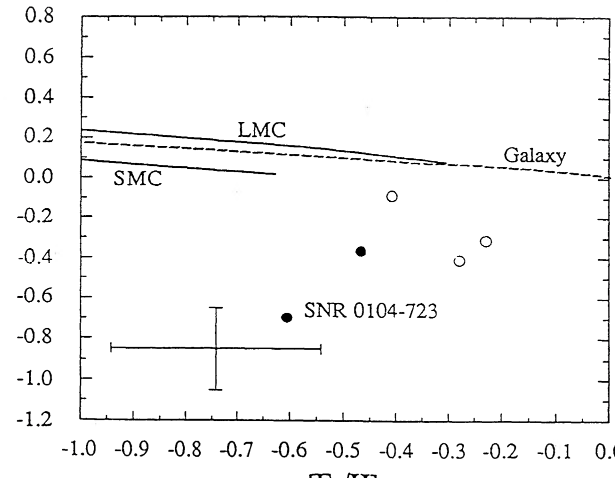

FIG. 6*b*

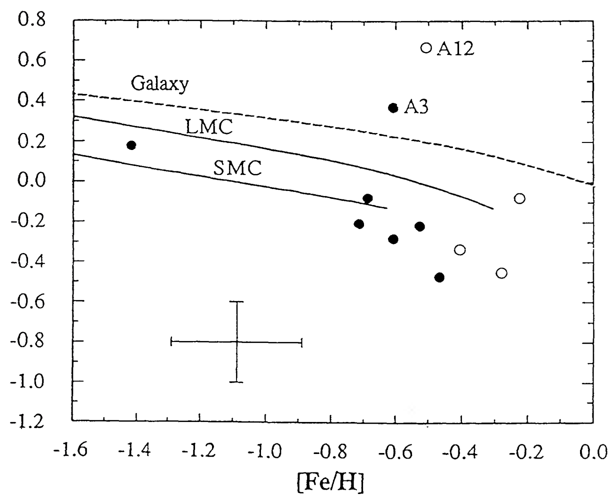

FIG. 6*c*

FIG. 6.—(*a*) Plot of the [C/Fe] ratio against [Fe/H] for the Galactic model (*dashed line*) and the Magellanic Cloud models (*solid lines as marked*). The data derived from Papers I and II are plotted here as open circles for the LMC and as closed circles for the SMC. An error bar of ± 0.2 dex is included to remind the reader of the scale and the typical sort of error to expect in the data. (*b*) Same as (*a*), but for the [N/Fe] ratio. (*c*) Same as (*a*), but for the [O/Fe] ratio.

τ_{defl}, however, the [α/Fe] ratio asymptotically approaches a common slope for all values of the time scale.

4. THE RELATIVE ABUNDANCE DISTRIBUTION OF THE ELEMENTS

4.1. *Carbon, Nitrogen, and Oxygen*

In Figures 6*a*–6*c* we plot against [Fe/H] the model results for the [C/Fe], [N/Fe], and [O/Fe] ratios, respectively. We have included in these diagrams data derived from Papers I and II (relative to the local Galactic ISM), and several sources from the literature. The filled circles represent data from the SMC, and the open circles are from the LMC. Owing to the incomplete coverage of the full range of elements observable in any one object, different objects are represented in each figure.

It may be seen from these graphs that, at the present levels of accuracy, we may consider the objects in both of the Clouds to form a continuous abundance series without introducing much additional error. Therefore, even though the objects studied reflect the present-day abundances of the local ISMs, in combination they may be considered in some sense as a single age sequence because of the relative star formation efficiencies of the Clouds.

In Figure 6*a* we have plotted the [C/Fe] ratios for the F supergiants we studied in Paper I, the F supergiants of Spite et al. (1989a), and the B stars (A3 and A12) from Reitermann et al. (1990). For these diagrams, and those that follow, we have included an error bar of ± 0.2 dex to give an indication of the scale of the most probable experimental error.

The models are in excellent agreement with the data to well within the experimental errors, although the only SNR that is included in this figure (N49 as marked) appears to be somewhat overdeficient in C (relative to Fe). This may well be due to survival of graphite grains in the recombination region of the SNR. Further information on the C abundances may be gained from Figure 7*a*, which shows the model results for [C/O] versus [O/H], and all the available observational data for these quantities in the Magellanic Clouds. Again we see that our models provide an excellent fit to these data. The supernova remnant N49 is observed to be overdeficient in C (relative to O), which suggests that it is indeed the carbon that is low, rather than both Fe and O that are high. Conversely, the two B stars studied by Reitermann et al. (1990) are observed to have a normal C abundance relative to Fe in Figure 6*a*, but a large underabundance of C relative to O in Figure 7*a*. This clearly indicates that it is the O abundance in these stars which is anomalously high. It will be interesting to see whether further analysis of these stars, and others like them, substantiates the high O abundances.

In conclusion, the excellent fit of our models to the C abundances (not specifically fitted in our derivation of the models) of the F supergiants expresses support for our models; more important, however, we believe that we have at last answered the question of why the C abundances in the Magellanic Clouds are apparently so very low (from the analysis of UV spectra of H II regions by Dufour et al. 1982 and Dufour et al. 1984). The answer seems to be that the C abundances are

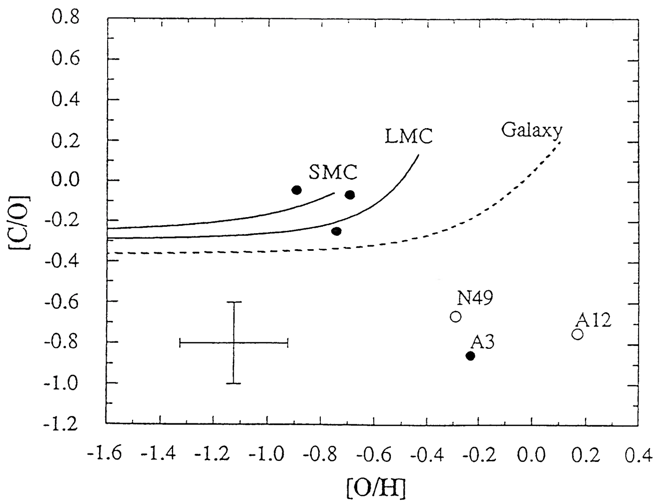

FIG. 7*a*

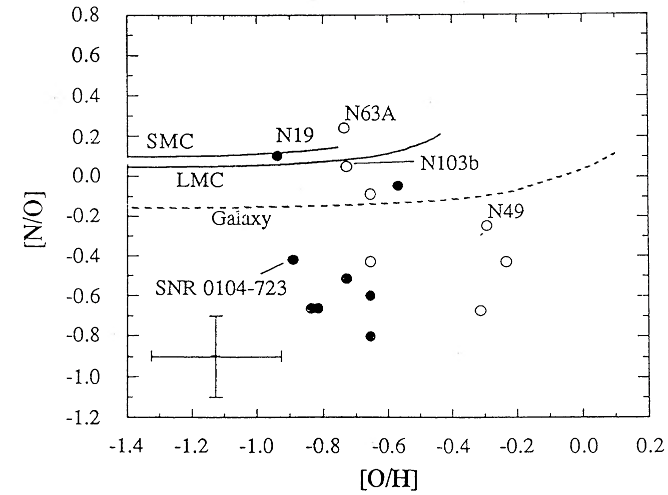

FIG. 7*b*

FIG. 7.—(*a*) Same as Fig. 6*a*, but for [C/O] plotted against [O/H]. (*b*) Same as Fig. 6*a*, but for [N/O] plotted against [O/H].

entirely normal in the Magellanic Clouds, and it is only the H II regions that are reflecting severe underabundances of C. These underabundances, then, are *intrinsic* to the H II regions, and an explanation for this must be sought in terms of such processes as the lockup of carbon onto graphite grains. These grains would have to have particle sizes somewhat larger than is common in our own Galaxy in order to account for the weakness of the 2200 Å absorption feature observed in the ISM of the Magellanic Clouds (see Koornneef & Code 1981; Bromage & Nandy 1983; Fitzpatrick & Savage 1984; Nandy, Morgan, & Houziaux 1984).

In Figure 6*b* we plot [N/Fe] against the [Fe/H] ratio for our models, and the data derived solely from the SNRs we studied in Paper II. Considering the severe underabundance of N found in most H II regions, our models fit all the SNR data, except SNR 0104−723, surprisingly well. The scatter increases somewhat when we turn to Figure 7*b*, where we plot the [N/O] ratio against [O/H] for both the SNRs (as marked) and the H II regions from Paper II. This is reminiscent of the scatter found in [N/O] for dwarf irregular galaxies (Dufour 1986; Matteucci & Tosi 1985), blue compact galaxies (see Pagel & Edmunds 1981 and references therein), the Galactic H II regions (Pagel 1985). However, it is still evident from Figure 7*b* that the SNRs are systematically more enhanced in N than are the H II regions. This may well be a modeling problem, but, if so, the cause remains obscure. More interestingly, we may be seeing a genuine difference between the N abundances in these types of objects. Either some process is depleting the N abundances observed in H II regions, or the SNR abundances are enhanced. Evidence for N enhancements in the atmospheres of massive stars is widespread (Luck & Lambert 1981), and, if ejected as a stellar wind, this material could pollute the surrounding ISM. Evidence that this may indeed happen comes from observations of nitrogen-rich knots in several SNRs, most notably Puppis A, and the observation of highly nitrogen-enriched ejecta around SN 1987A (Kirshner 1988; Fransson et al. 1989).

Many suggestions have been put forward in recent years to explain the observed spread in [N/O]. Matteucci & Chiosi (1983), for instance, suggested that the spread in N and O abundances with the fractional gas mass, M_{gas}/M_{tot}, might be due to variations from galaxy to galaxy in (1) the IMF and/or the chemical yields, (2) the infall rate/SFR ratio, and (3) the rate of mass outflow/SFR ratio; Matteucci & Tosi (1985), on the other hand, suggest that the spread may be explained by a variation in the galactic wind/SFR ratio from galaxy to galaxy.

Similarly, many authors (for example, Alloin et al. 1979; Pagel & Edmunds 1981; Serrano & Peimbert 1983) have endeavored to explain the spread in the [N/O] ratio in terms of differing contributions of primary and secondary nitrogen. Matteucci & Tosi (1985) suggests that it is due to variations in the ambient metallicity affecting the limiting mass, M_{up}, required for accumulating degenerate carbon cores and thereby affecting the mass range of stars capable of producing primary nitrogen. In addition, Tosi (1988) showed that N is strongly reduced in abundance when the effects of overshooting are included, owing to the reduction in the stellar envelopes as the core size is increased and to the decrease in the mass range of stars experiencing envelope burning (see Greggio & Tosi 1986). In the LMC and the SMC, however, the massive Type I planetary nebulae are observed to be rich in nitrogen (Meatheringham & Dopita 1991a, b). Since dredge-up processes are responsible for this, the nitrogen in these cases may be regarded as primary. Other uncertainties, such as the rate of the $^{12}C(\alpha, \gamma)^{16}O$ reaction (we have assumed the standard rate throughout), could also have a significant influence on how the N abundance might vary from one environment to another (see Matteucci 1986 for a discussion of the consequences of adopting the higher rate put forward by Kettner et al. 1982).

In conclusion, the production mechanisms for nitrogen are still highly controversial, both observationally and theoretically. Until they are determined, nitrogen will remain a poor diagnostic for the determination of the general features of the star formation histories of galaxies, but clearly the nitrogen abundance is telling us a lot about the formation and evolution of intermediate-mass stars.

In Figure 6*c* we show our model results for the [O/Fe] ratio plotted against [Fe/H], superposed on the observational data available to us. These data are derived from all of the SNRs we studied in Paper II; the three F supergiants and one red supergiant studied by Spite et al. (1989b) and Spite et al. (1986), respectively; and the two B stars studied by Reitermann et al. (1990). Again the B stars are relatively overabundant in oxygen, but our models fit all the other data remarkably well, thus adding support to the validity of the models (the models having been forced to fit the H II region O abundances, which could not be displayed in this figure).

4.2. *The α-Elements*

The α-elements are defined as those which have been built by α-particle addition to seed nuclei, and therefore have an even number of protons and neutrons in the nuclei of their major isotope. Most workers agree that the elements O, Ne, Mg, Si, S, and Ca belong to this group, but Ti has sometimes been excluded. Certainly a part of the Ti abundance is contributed through the α-process, while the rest probably results from the equilibrium burning to the iron-peak elements. However, the [Ti/Fe] ratio appears to act like an α-element in its variation with Fe abundance (see Magain 1989), so the contribution from the equilibrium process must be quite small. Woosley & Hoffman (1991) have shown that the abundance of ^{44}Ti can be understood as a consequence of α-rich freezeout in Type II supernovae. On this basis, Ti is included here as a member of the α-process elements. (See also the review by Wheeler et al. 1989.)

Since the α-elements are produced by Type II supernovae of massive stars, while the bulk of Fe is derived from deflagration of C-O white dwarfs on a much longer time scale, the ratio of the α-element abundance to Fe compared with solar puts interesting constraints on the past history of low-mass to high-mass star formation.

In Figure 8 we plot the combined contributions of the three well-observed α-elements in our data according to the formula

$$[\alpha/\mathrm{Fe}] = 1/3([\mathrm{Mg/Fe}] + [\mathrm{Ca/Fe}] + [\mathrm{Ti/Fe}])\ ,$$

where at least two elements have been used in determining the average; when one is missing, the mean of the average differences between that element and the other two is substituted. In addition, we have plotted our model results for the [O/Fe] ratio, which, as discussed previously, follows the trends of the other α-elements closely. We see that the models fit the data within the experimental errors, although there may be an indication that they underestimate the α-abundances by 0.1–0.2 dex. Since the models have been fitted to the O abundances, this would indicate that the other α-elements are overabundant relative to O in the Clouds, which is perhaps the result of the different stellar mass ranges responsible for the bulk of each individual element. Indeed, variations of this order between different α-elements is a feature of the Galactic abundances in this metallicity range (see Andersen et al. 1988).

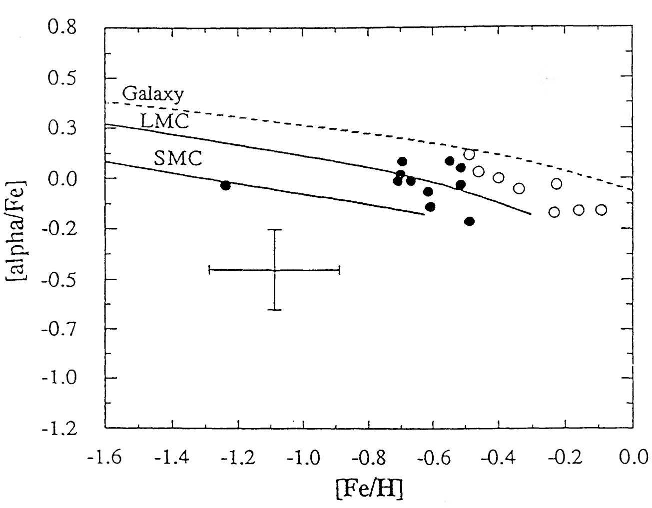

FIG. 8.—Same as Fig. 6*a*, but for the [α-elements/Fe] ratio, where the α-elements are defined in the text.

The most obvious feature apparent in both Figures 6*c* and 8 is the systematically lower [α/Fe] ratio observed in the Clouds relative to the Galaxy. As discussed in § 2, the evolution of this ratio with metallicity is driven by the slope of the IMF, the infall time scale, and the deflagration time scale. As may be seen from Table 2, our results indicate that it is not the latter time scale that could be responsible for the lower ratio in the Clouds, since it is *longer* in the Clouds than in the Galaxy, which would give a lower Fe abundance and thus a higher [α/Fe] ratio. The infall time scale for each of the Clouds is also substantially longer than for the Galaxy, again having a result in the opposite sense to the one observed. It appears, therefore, that the steeper slope of the IMF is the critical factor in reducing the [α/Fe] ratio, through the relative decrease in the numbers of massive stars.

This agrees with the observational results on the slope of the upper IMF in the Clouds by Humphreys & McElroy (1984). One possible way to explain such a steep IMF compared with that of the Galaxy is to appeal to the differences in the global structures of the Clouds and the Galaxy. Shearing motions in the disks of both the LMC and the SMC must be low, since their rotation velocities are low and they both have large areas of solid-body rotation. It follows that their molecular clouds will experience fewer high-velocity collisions and will be more prone to low-velocity coalescence. Under such conditions, we speculate that fragmentation will take place under cooler conditions than in the more violent conditions experienced in the Galaxy and the other spiral galaxies, resulting in fewer high-mass stars and, therefore, a steeper IMF on average.

An alternative explanation for the low [α/Fe] ratio has been proposed by Matteucci (1990) and independently by Gilmore & Wyse (1991). These authors propose that dwarf galaxies suffer bursts of star formation separated by long periods of quiescence. Then, with a somewhat larger fraction of deflagration supernovae, the [O/Fe] ratio need no longer be monotonically decreasing with time but can increase again near bursts. Some evidence in support of this viewpoint is the apparent absence of intermediate-age clusters in the Magellanic Clouds (da Costa 1990). However, the field stars do not appear to show a corresponding deficit, and the LMC appeared to be continuously enriching itself over this period. Thus, although the hypothesis of episodic star formation is interesting, we must await more detailed studies of the star formation history of the LMC before this point can be definitively addressed.

4.3. *The Odd Elements*

We include in this section the odd elements Na and Al. These lie below those of the Fe-peak group in atomic mass, and we have little information on their abundances at present. For Na, the combined analyses of our own work (Paper I), Spite et al. (1986), and Spite et al. (1989b) give us information on a total of six stars, which is only sufficient to show that their abundances relative to Fe are no different from that of the solar vicinity, within the experimental errors. For Al the situation is worse, since there are data for only one star (from Spite et al. 1989b).

The odd elements of the Fe peak comprise Sc, V, Mn, Co, and Cu, and they owe their existence to neutron irradiation of seed nuclei during the major stellar burning phases. The abundances are therefore highly dependent on the neutron flux and the interior temperatures of stars, as well as on the abundances of the seed nuclei. Accordingly, these elements have the potential for acting as sensitive probes of the temperatures of stellar interiors. Unfortunately, the fact that all these elements have unpaired protons means that they all experience hyperfine splitting (HFS) of their energy levels resulting from the presence of a nuclear magnetic moment. Little effort has been put into correcting for the HFS in the past (except for the case of Mn, which has been studied carefully by Beynon 1978a, b and Gratton 1989), so it is still uncertain how the abundances vary in our own Galaxy. Instead of using precise oscillator strengths (often not available for the transition of interest anyway), most workers have relied on empirical corrections to the turbulent velocity ξ_{turb} in deriving the abundances. This is clearly unsatisfactory, as shown by the large scatter in abundances derived from stars from different sources (Lambert 1989; Wheeler et al. 1989). In Paper I we also used an empirical technique to estimate the extra ξ_{turb} required to correct for the HFS, based on some careful work by Gratton (1982) and the Liège solar atlas. However, since we measured our abundances differentially with respect to Canopus, any errors in the HFS correction should canel out.

In Figures 9*a*–9*c* we plot [Sc/Ti], [V/Cr], and [Mn/Fe], respectively, against the Fe abundance [Fe/H]. That is, we plot the ratios of the odd elements, with their nearest neighboring even elements, to see whether there is any sign of an odd-even effect. We see immediately that there is no obvious effect for Sc or Mn, while V is apparently overabundant.

In the field stars of the Galaxy, Sc and V are believed to be invariant relative to Fe with decreasing metallicity (Wheeler et al. 1989); however, the lack of accurate HFS corrections weakens these conclusions. The globular clusters, on the other hand, display a systematic overabundance of ~ 0.25 dex in [V/Fe] (Wheeler et al. 1989 and references therein). This may be an indication that the process acting to enhance the V abundance in the Galactic globular clusters is also of importance in the Magellanic Clouds.

The relative Mn abundances in the solar neighborhood of our Galaxy shows some sign of decreasing for [Fe/H] $< \sim -0.4$. Considering the scatter in our abundances, we cannot rule out a similar drop in the relative Mn abundances for the Magellanic Clouds.

We may conclude that our observations for all three elements are in substantial agreement with the Galactic results, except that V may be somewhat overproduced relative to the field stars.

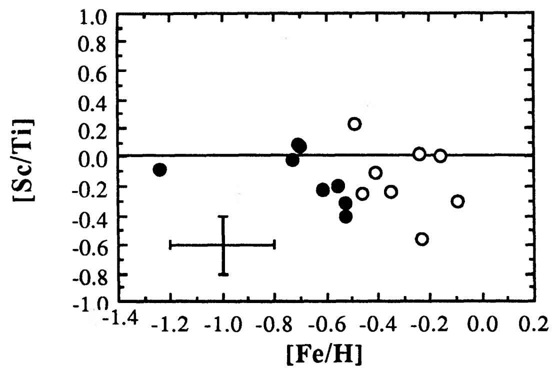

FIG. 9*a*

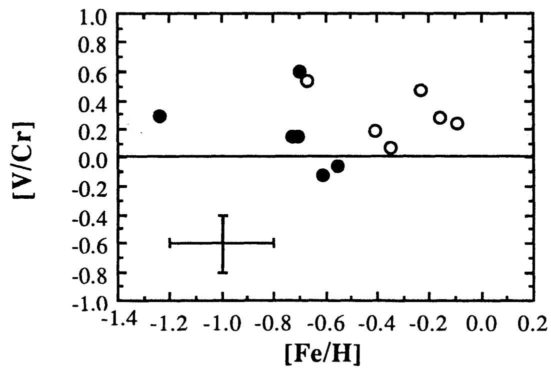

FIG. 9*b*

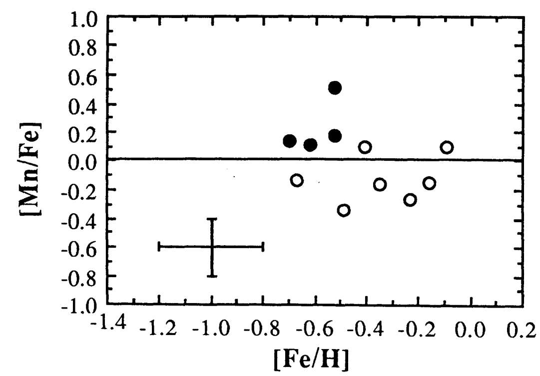

FIG. 9*c*

FIG. 9.—(*a*) Odd-even closest neighbors [Sc/Ti] plotted against [Fe/H], for the LMC (*open circles*) and the SMC (*closed circles*). As for the previous figures, a 0.2 dex error bar has been included as an indication of the errors and the scale. (*b*) Same as (*a*), but for [V/Cr]. (*c*) Same as (*a*), but for [Mn/Fe].

4.4. *The Even* Fe-*Peak Elements*

The only two elements that we consider in this category, besides Fe itself, are Cr and Ni. The relative abundances of these elements are plotted against [Fe/H] in Figures 10*a* and 10*b*, where it is evident that both elements deviate little from proportional production with iron. Most of the evidence in the literature agrees that this is also the case for the Galaxy, and since these elements, together with Fe, are formed in the nuclear statistical equilibrium process during supernova explosions of both Type I and Type II, it would indeed be surprising if their abundances did not correlate as well as they do.

4.5. *The Neutron Capture Elements*

Except for Zn and certain rare isotopes, the only processes capable of building heavier elements beyond the Fe peak are the slow (*s*-process) or rapid (*r*-process) neutron capture reactions. The *s*-process elements are thought to be produced by two different mass ranges of stars. The so-called main component with $A \geq 89$ is produced mainly by intermediate-mass

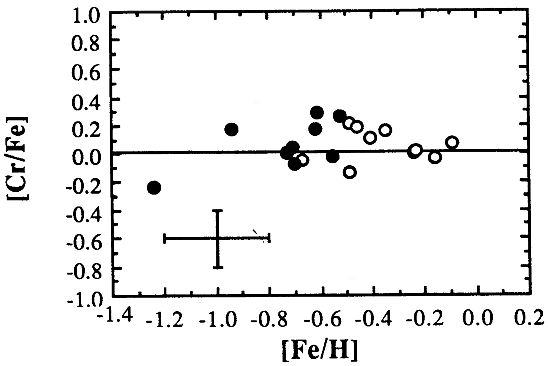

FIG. 10*a*

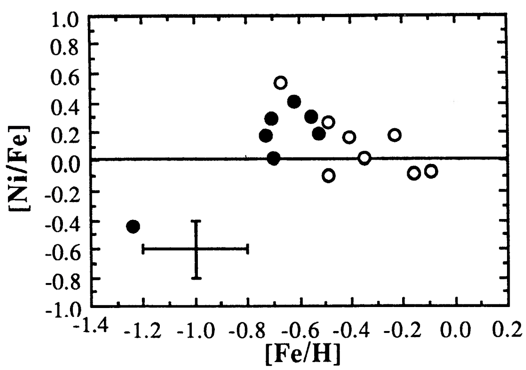

FIG. 10*b*

FIG. 10.—(*a*) Even iron-peak element ratio [Cr/Fe] plotted against [Fe/H]. The LMC (*open circles*) and the SMC (*closed circles*) are plotted, and, as for the previous figures, a 0.2 dex error bar has been included as an indication of the errors and the scale. (*b*) Same as (*a*), but for [Ni/Fe].

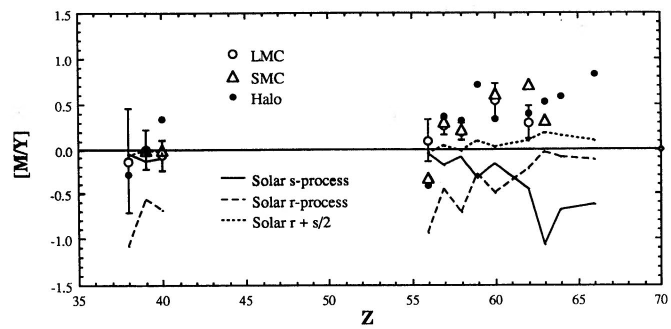

FIG. 11*a*

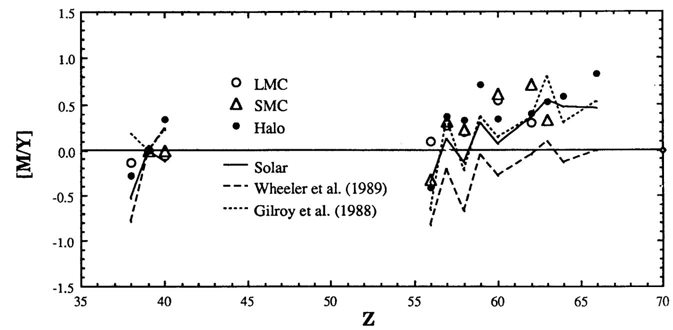

FIG. 11*b*

FIG. 11.—(*a*) [M/Y] from the Galactic halo (*closed circles*), the SMC (*open triangles*), and the LMC (*open circles*) plotted against *Z*. The solid and the long-dashed lines represent the contributions from the *s*-process and the *r*-process, respectively, to the solar abundances, normalized so that their sum is equal to zero. The short dashed line represents the sum of the *r*-process and half the *s*-process contributions to the solar abundances, normalized at Y. The error bars for the LMC, due only to the observed scatter in the abundances (see Paper I), are included in this diagram for illustrative purposes. (*b*) Same as (*a*), except that the solid line is the solar *r*-process contribution, the long dashes are due to the *r*-process model of Wheeler et al. (1989), while the short dashes are due to the *r*-process model of Gilroy et al. (1988). See (*a*) for illustrative error bars.

stars during the thermally pulsing (TP) phase of their evolution up the asymptotic giant branch (AGB). The neutron source is thought to be mainly the $^{13}C(\alpha, n)^{16}O$ reaction, with a small contribution from the $^{22}Ne(\alpha, n)^{25}Mg$ reaction (see Käppeler et al. 1990). For the "weak component" with $A < 89$, the neutron source is the $^{22}Ne(\alpha, n)^{25}Mg$ reaction alone in massive stars ($M/M_{\odot} > 10$) near the end of core helium burning (see Prantzos, Hashimoto, & Nomoto 1990).

In 1981, Truran proposed that, for extremely metal-weak halo stars ([Fe/H] < -2.0), *only* the *r*-process reactions have contributed to the abundances of the neutron capture elements. This has received some support in recent years (Gilroy et al. 1988; Wheeler et al. 1989), through comparing the observed abundance patterns for the neutron capture elements with the theoretical abundance patterns produced solely by the *r*-processes.

We have plotted in Figure 11*a* the Magellanic Cloud [M/Y] abundance patterns for the observable elements heavier than $Z = 37$. Included on this diagram are the average of the halo star abundances used by Gilroy et al. (1988) and Wheeler et al. (1989), and superposed on these we have added the *r*- and *s*-process contributions to the solar abundances derived by Cameron (1982a). We have also computed a model whereby the full *r*-process contribution to the solar system has been added to half of the *s*-process contribution, and the result has been normalized to zero at Y. The normalizing point at Y ($Z = 39$) was chosen because this element seems to be in relatively constant proportion to Fe.

None of these curves fit either the Galactic halo or the Magellanic Clouds. From this we may conclude that the neutron processing histories of the Clouds and the Galactic halo have been markedly different from that of the Sun. Even a 50% increase in the contribution by the *r*-process relative to the *s*-process is insufficient to account for the observations. However, it is also apparent that any combination of *s*- and *r*-processes that includes at least half the solar *s*-process contribution would fit the Magellanic Cloud data for the light neutron capture elements (Sr, Y, Zr), whereas the Galactic halo has an entirely different distribution of these elements.

In Figure 11*b* we superpose on the data the solar *r*-process contributions from Cameron (1982a) and the two *r*-process models derived from Gilroy et al. (1988) and Wheeler et al. (1989), respectively. We see from this that the solar *r*-process contributions and the model due to Gilroy et al. (1988) fit the observed abundance distribution beyond $Z = 55$, for both the Galactic halo *and the Magellanic Clouds*, at least qualitatively. Indeed, there is little obvious difference between the distribution of the Clouds and the halo in this range of elements, except perhaps a high Ba abundance in the LMC, which suggests a normal contribution from the *s*-process for this element.

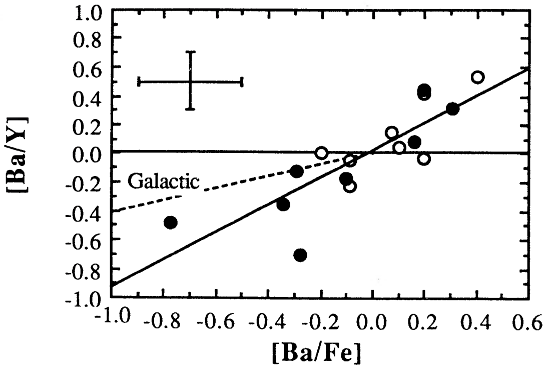

FIG. 12.—[Ba/Y] ratio plotted against [Ba/Fe] for the LMC (*open circles*) and the SMC (*closed circles*). The dashed line is the result for the Galaxy derived by Spite & Spite (1978). A 0.2 dex error bar has been included as an indication of the errors and the scale.

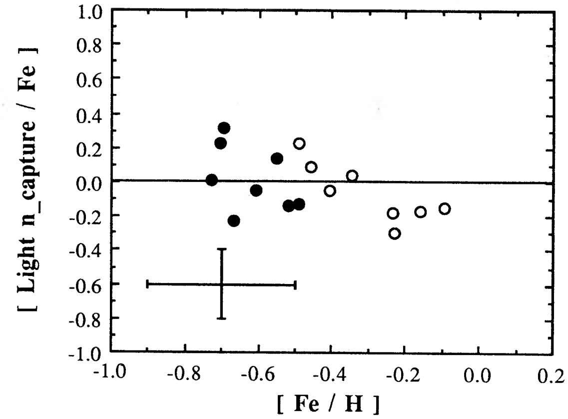

FIG. 13*a*

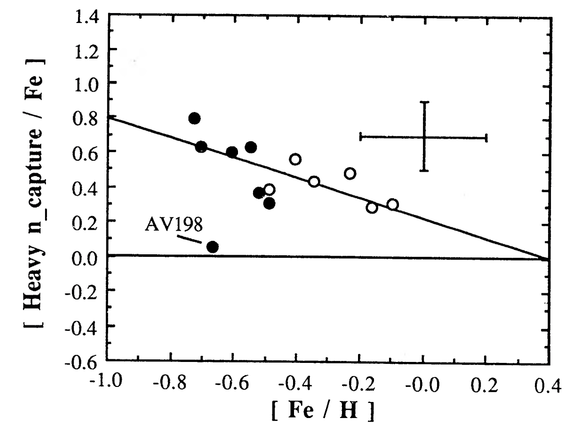

FIG. 13*b*

FIG. 13.—(*a*) [Light neutron capture elements/Fe] plotted against [Fe/H] for the LMC (*closed circles*) and the SMC (*open circles*). A 0.2 dex error bar has been included as an indication of the errors and the scale. (*b*) Same as Fig. 11*a*, but for the [heavy neutron capture elements/Fe].

It seems, therefore, that there has perhaps been a significant additional *r*-process component to the elemental abundances in the Magellanic Clouds. However, this could not have been due to a larger number of massive stars in the Clouds than in our Galaxy, or it would have resulted in an overproduction in the α-elements.

In Figure 12 the [Ba/Y] ratio is plotted against [Ba/Fe] for the Clouds, together with a least-squares fit and the line that best fits the Galactic data (from Spite & Spite 1978). It appears that the [Ba/Y] ratio might fall more steeply with decreasing Ba abundance in the Clouds than in the Galaxy. The reason for the fall is that Ba requires a higher neutron irradiation than Y for its formation. These results indicate that the neutron irradiation in the intermediate-mass stars in the Clouds may have been lower than in our own Galaxy. This may contribute to the apparent *r*-process–dominated abundance pattern for the heavy elements in the Clouds.

In Figures 13*a* and 13*b* we plot the average light neutron capture and heavy neutron capture abundances, respectively, against [Fe/H]. The light neutron capture elements are defined here to be half the sum of the Y and Zr abundances relative to Fe for those stars where both were measured, while the heavy neutron capture abundances, $[M_{hn}/Fe]$, are defined here to be

$$[M_{hn}/Fe] = \tfrac{1}{4}([La/Fe] + [Ce/Fe] + [Nd/Fe] + [Sm/Fe]) ,$$

where at least two elements were measured from any star. Those for which we had no data were replaced with values maintaining the average abundance difference observed between that element and Ce. The light neutron capture elements show no obvious deviation from strict proportionality to [Fe/H]. For the heavy neutron capture elements, however, except for the apparently discrepant point from AV 198 (see Paper I), the points define a remarkably tight relationship of *decreasing* relative abundance with increasing [Fe/H]. This is in contrast to the strict proportionality with Fe found in the Galaxy at these metallicities (Luck & Bond 1985; Magain 1989), and suggests again that the heavy elements in the Clouds are produced by massive stars (and hence the *r*-process), with little contribution from the intermediate-mass stars.

5. SUMMARY AND FUTURE WORK

In this work we have established four major results:

1. The interstellar medium of the LMC has a mean metallicity 0.2 dex lower than the local ISM, and the metallicity of the SMC is 0.6 dex lower. However, the interstellar media of both the Magellanic Clouds and the Galaxy have significantly nonsolar elemental ratios.

2. The stellar carbon abundances in the Clouds appear to be entirely normal; it is therefore the H II regions that must be overdeficient in this element.

3. The light-element abundances of the local Galactic ISM are systematically *less* than those of the Sun, despite the fact that the Sun is already ∼4 Gyr old. One possible explanation for this is that there has been a radial inflow of the ISM with respect to the Sun through stellar orbital diffusion.

4. The *s*-process appears to have been less effective, and the *r*-process more effective, in the Magellanic Clouds at producing heavy neutron capture elements, when compared with the Galaxy.

There is, of course, much room for improvement in this first analysis of the detailed global abundances in the Magellanic Clouds. Many critical elements need to be studied more carefully (Na, Si, S, Sr, Ba, and Eu), while others have not been observed at all (Al, Gd, and Dy). The sample of objects is sometimes embarrassingly small (for example, only two SNRs were observed in the SMC). The possibility of observing some of the lighter elements by studying near–main-sequence B stars opens up a whole new field of study. This work is all within the reach of present-day ground-based observations; however, with the launch of the *Hubble Space Telescope*, new possibilities present themselves. We are now capable of taking spectra of fainter, and therefore older, stars in the Magellanic Clouds, thus providing a longer baseline for investigating the star formation history of the Clouds.

This study has opened up a range of questions that can be answered properly only through more detailed theoretical modeling in conjunction with further observations. In particular, we identify the following: What causes the variations in production efficiencies of the *s*-process and *r*-process elements? Why is nitrogen anomalously underabundant in the H II regions, and yet almost of normal abundance relative to iron in the SNRs? Why are the carbon abundances in the H II regions overdeficient? Does the IMF or variation in the star formation rate principally determine the evolution of the [O/Fe] ratio? Why is vanadium apparently overproduced in the Clouds?

Investigation of these questions will have to be left as the subjects of future papers.

Thanks to all those who have helped in making the observations, and to the Directors and staff of both Mount Stromlo and Siding Spring Observatories and the Anglo-Australian Observatory, for the use of their facilities. The Australian Time Allocation Committee has been generous in their support for this project, which is gratefully acknowledged. Thanks also to Mike Bessell, Graeme Smith, Peter Wood, and Bernard Pagel for their helpful comments and suggestions. Finally, one of us (S. C. R.) would like to acknowledge the financial support received from a Commonwealth Postgraduate Scholarship during the course of this work.

REFERENCES

Alloin, D., Collin-Souffrin, S., Joly, M., & Vigroux, L. 1979, A&A, 78, 200
Anders, E., & Grevesse, N. 1989, Geochim. Cosmochim. Acta, 53, 197
Andersen, J., Edvardsson, B., Gustafsson, B., & Nissen, P. E. 1988, in IAU Symp. 132, The Impact of Very High S/N Spectroscopy on Stellar Physics, ed. G. Cayrel de Strobel & M. Spite (Dordrecht: Kluwer), 441
Arnett, D. W. 1978, ApJ, 219, 1008
Audouze, J., Chiosi, C., & Woosley, S. E. 1986, Nucleosynthesis and Chemical Evolution (Sauverny-Versoix: Geneva Observatory)
Augarde, R., & Lequeux, J. 1985, A&A, 147, 273
Beynon, T. G. R. 1978a, A&A, 64, 145
———. 1978b, A&A, 64, 299
Bica, E., Dottori, H., & Pastoriza, M. 1986, A&A, 156, 261
Binette, L., Dopita, M. A., & Tuohy, I. R. 1985, ApJ, 297, 476
Blackwell, D. E., Shallis, M. J., & Simmons, G. J. 1982, MNRAS, 199, 37
Branch, D., & Nomoto, K. 1986, A&A, 164, L13
Bromage, G. E., & Nandy, K. 1983, MNRAS, 204, 29P
Burki, G. 1977, A&A, 57, 135
Butcher, H. R. 1977, ApJ, 216, 373
Cameron, A. G. W. 1982a, Ap. Space Sci., 82, 123
———. 1982b, in Essays in Nuclear Astrophysics, ed. C. A. Barnes, D. D. Clayton, & D. N. Schraam (Cambridge: Cambridge Univ. Press), 23
Castellani, V., Chieffi, A., Pulone, L., & Tornambè, A. 1985, ApJ, 294, L31
Chièze, J.-P. 1987, A&A, 171, 225
da Costa, G. S. 1990, in IAU Symp. 148, The Magellanic Clouds and Their Dynamical Interaction with the Milky Way, ed. D. K. Milne & R. F. Haynes (Dordrecht: Kluwer), 183
Desikachary, K., & Hearnshaw, J. B. 1982, MNRAS, 201, 707
Donas, J., & Deharveng, J. M. 1984, A&A, 140, 325
Dopita, M. A. 1985, ApJ, 295, L5
———. 1987, in IAU Symp. 115, Star Forming Regions, ed. M. Peimbert & J. Jugaku (Dordrecht: Reidel), 501
———. 1990, in The Interstellar Medium in Galaxies, ed. H. A. Thronson & J. M. Shull (Dordrecht: Kluwer), 437
Dopita, M. A., & Meatheringham, S. J. 1991, ApJ, 367, 115
———. 1991b, ApJ, 377, 480
Dufour, R. D. 1984, in IAU Symp. 108, Structure and Evolution of the Magellanic Clouds, ed. S. van den Bergh & K. S. de Boer (Dordrecht: Reidel), 353
———. 1986, PASP, 98, 1025
Dufour, R. J., Schiffer, F. H., & Shields, G. A. 1984, in The Future of Ultraviolet Astronomy Based on Six Years of *IUE* Research (NASA CP-2349), 111
Dufour, R. J., Shields, G. A., & Talbot, R. J., Jr. 1982, ApJ, 252, 461
Evans, I. N., & Dopita, M. A. 1985, ApJS, 58, 125
Filippenko, A. V., & Sargent, W. L. W. 1986, AJ, 91, 691
Fitzpatrick, E. L., & Savage, B. D. 1984, ApJ, 279, 578
Franco, J. 1983, ApJ, 264, 508
Franco, J., & Cox, D. P. 1983, ApJ, 273, 243
Fransson, C., Cassatella, A., Gilmozzi, R., Kirshner, R. P., Panagia, N., Sonneborn, G., & Wamsteker, W. 1989, ApJ, 336, 429
Frantsman, J. L. 1988, Ap. Space Sci., 145, 287
Frogel, J. A., & Blanco, V. M. 1983, ApJ, 274, L57
Gaskell, C. M., Cappellaro, E., Dinerstein, H. L., Garnett, D. R., Harkness, R. P., & Wheeler, J. C. 1986, ApJ, 306, L77
Gilmore, G., & Wyse, R. F. G. 1991, ApJ, 367, L55
Gilroy, K. K., Sneden, C., Pilachowski, C. A., & Cowan, J. J. 1988, ApJ, 327, 298
Gratton, R. G. 1982, ApJ, 257, 640
———. 1989, A&A, 208, 171
Greggio, L., & Tosi, M. 1986, A&A, 156, L1
Güsten, R., & Mezger, P. G. 1983, Vistas Astron., 26, 159
Hawkins, M. R. S., & Brück, M. T. 1982, MNRAS, 198, 935
Hawkins, M. R. S., & Brück, M. T. 1984, in IAU Symp. 108, Structure and Evolution of the Magellanic Clouds, ed. S. van den Bergh & K. S. de Boer (Dordrecht: Reidel), 353
Humphreys, R. M., & McElroy, D. B. 1984, ApJ, 284, 565
Hunter, D. A., Gallagher, J. S., & Rautenkranz, D. 1982, ApJS, 49, 53
Iben, I., Jr., Nomoto, K., Tornambè, A., & Tutukov, A. 1987, ApJ, 317, 717
Iben, I., Jr., & Tutukov, A. V. 1984, ApJS, 54, 335
———. 1985, ApJS, 58, 661
Israel, F. P. 1984, in IAU Symp. 108, Structure and Evolution of the Magellanic Clouds, ed. S. van den Bergh & K. S. de Boer (Dordrecht: Reidel), 319
Käppeler, F., Gallino, R., Busso, M., Picchio, G., & Raiteri, C. M. 1990, ApJ, 354, 630
Kettner, K. U., et al. 1982, Z. Phys., A308, 73
Kirshner, R. P. 1988, in IAU Colloq. 108, Atmospheric Diagnostics of Stellar Evolution: Chemical Peculiarity, Mass Loss, and Explosion, ed. K. Nomoto (Berlin: Springer), 252
Koornneef, J., & Code, A. D. 1981, ApJ, 247, 860
Lambert, D. L. 1989, in Cosmic Abundances of Matter, ed. C. S. Waddington (New York: AIP), 168
Larson, R. B. 1981, MNRAS, 194, 809
———. 1985, MNRAS, 214, 379
———. 1986, MNRAS, 218, 409
Lequeux, J. 1979, A&A, 71, 1
———. 1984, in IAU Symp. 108, Structure and Evolution of the Magellanic Clouds, ed. S. van den Bergh & K. S. de Boer (Dorderecht: Reidel), 67
Luck, R. E., & Bond, H. E. 1985, ApJ, 292, 559
Luck, R. E., & Lambert, D. L. 1981, ApJ, 245, 1018
Lyubimkov, L. S., & Boyarchuk, A. A. 1982, Astrofizika, 18, 596
Magain, P. 1989, A&A, 209, 211
Mathewson, D. S., & Ford, V. L. 1984, in IAU Symp. 108, Structure and Evolution of the Magellanic Clouds, ed. S. van den Bergh & K. S. de Boer (Dordrecht: Reidel), 125
Matteucci, F. 1986, ApJ, 305, L81
———. 1990, in IAU Symp. 143, Wolf-Rayet Stars and Interrelations with Other Massive Stars in Galaxies, ed. K. A. van der Hucht & B. Hidayat (Dordrecht: Kluwer), 625
Matteucci, F., & Chiosi, C. 1983, A&A, 123, 121
Matteucci, F., & Greggio, L. 1986, A&A, 154, 279
Matteucci, F., & Tornambè, A. 1985, A&A, 142, 13
Matteucci, F., & Tosi, M. 1985, MNRAS, 217, 391
Meatheringham, S. J., & Dopita, M. A. 1991a, ApJS, 75, 407
———. 1991b, ApJS, 76, 1085
Nandy, K., Morgan, D. H., & Houziaux, L. 1984, MNRAS, 211, 895
Nomoto, K. 1984, in Stellar Nucleosynthesis, ed. C. Chiosi & A. Renzini (Dordrecht: Reidel), 239
Nomoto, K., Thielemann, F. K., & Yokoi, Y. 1984, ApJ, 286, 644
Norman, C., & Silk, J. 1980, ApJ, 238, 158
Olofsson, K., Bergvall, N., & Ekman, A. 1984, A&A, 137, 327
Pagel, B. E. J. 1985, in ESO Workshop 21, Production and Distribution of CNO Elements, ed. I. J. Danziger, F. Matteucci, & K. Kjär (Garching: ESO), 155
———. 1988, in Evolutionary Phenomena in Galaxies, ed. J. Beckman & B. E. J. Pagel (Cambridge: Cambridge Univ. Press), 201
Pagel, B. E. J., & Edmunds, M. G. 1981, ARA&A, 19, 77
Pagel, B. E. J., Edmunds, M. G., Fosbury, R. A. E., & Webster, B. L. 1978, MNRAS, 184, 569
Peimbert, M. 1987, in IAU Symp. 115, Star Forming Regions, ed. M. Peimbert & J. Jugaku (Dordrecht: Reidel), 111
Prantzos, N., Hashimoto, M., & Nomoto, K. 1990, A&A, 234, 211
Reitermann, A., Baschek, B., Stahl, O., & Wolf, B. 1990, A&A, 234, 109

Renzini, A., Bernazzani, M., Buonanno, R., & Corsi, C. E. 1985, ApJ, 294, L7
Renzini, A., & Voli, M. 1981, A&A, 94, 175
Reynolds, S. E., Hearnshaw, J. B., & Cottrell, P. L. 1988, MNRAS, 235, 1423
Rieke, G. H., Cutri, R. M., Black, J. H., Kailey, W. F., McAlary, C. W., Lebofsky, M. J., & Elston, R. 1985, ApJ, 290, 116
Rieke, G. H., Lebofsky, M. J., Thompson, R. I., Low, F. J., & Tokunaga, A. T. 1980, ApJ, 238, 24
Russell, S. C., & Bessell, M. S. 1989, ApJS, 70, 865 (Paper I)
Russell, S. C., & Dopita, M. A. 1990, ApJS, 74, 93 (Paper II)
Scalo, J. M. 1986, Fund. Cosmic Phys., 11, 1
Scoville, N. Z., & Good, J. C. 1989, ApJ, 339, 149
Scoville, N. Z., Sanders, D. B., & Clemens, D. P. 1986, ApJ, 310, L77
Serrano, A., & Peimbert, M. 1983, Rev. Mexicana Astron. Af., 8, 117
Shaver, P. A., McGee, R. X., Newton, L. M., Danks, A. C., & Pottasch, S. R. 1983, MNRAS, 204, 53
Sneden, C. 1985, in ESO Workshop 21, Production and Distribution of CNO Elements, ed. I. J. Danziger, F. Matteucci, & K. Kjär (Garching: ESO), 1
Spite, M., Barbuy, B., & Spite, F. 1989a, A&A, 222, 35
Spite, M., Cayrel, R., François, P., Richtler, T., & Spite, F. 1986, A&A, 168, 197
Spite, M., & Spite, F. 1978, A&A, 67, 23
Spite, F., Spite, M., & François, P. 1989b, A&A, 210, 25
Stryker, L. L. 1981, Ph.D. thesis, Yale Univ.
Stryker, L. L., & Butcher, H. R. 1981, in IAU Colloq. 68, Astrophysical Parameters for Globular Clusters, ed. A. G. D. Philip & D. S. Hayes (Schenectady: Davis), 255
Thielemann, F. K., & Arnett, D. W. 1985, ApJ, 295, 604
Thielemann, F. K., Nomoto, K., & Yokoi, K. 1986, A&A, 158, 17
Tornambè, A., & Matteucci, F. 1987, ApJ, 318, L25
Tosi, M. 1988, A&A, 197, 33
Tosi, M., & Diaz, A. 1985, MNRAS, 217, 571
Truran, J. W. 1981, A&A, 97, 391
van den Bergh, S., McClure, R. D., & Evans, R. 1987, ApJ, 323, 44
Wheeler, J. C., Sneden, C., & Truran, J. W., Jr. 1989, ARA&A, 27, 279
Whelan, J. C., & Iben, I., Jr. 1973, ApJ, 186, 1007
Woosley, S. E., & Hoffman, R. D. 1991, ApJ, 368, L31
Woosley, S. E., & Weaver, T. A. 1982, in Essays on Nuclear Astrophysics, ed. C. A. Barnes, D. D. Clayton, & D. Schramm (Cambridge: Cambridge Univ. Press), 377
———. 1986, ARA&A, 24, 205
Wyse, R. F. G., & Silk, J. 1989, ApJ, 339, 700